



HAL
open science

Sampling of suspended particulate matter using particle traps in the Rhône River: Relevance and representativeness for the monitoring of contaminants

M. Masson, H. Angot, C. Le Bescond, M. Launay, Aymeric Dabrin, Cecile Miege, Jérôme Le Coz, Marina Coquery

► To cite this version:

M. Masson, H. Angot, C. Le Bescond, M. Launay, Aymeric Dabrin, et al.. Sampling of suspended particulate matter using particle traps in the Rhône River: Relevance and representativeness for the monitoring of contaminants. *Science of the Total Environment*, 2018, 637-638, pp.538-549. 10.1016/j.scitotenv.2018.04.343 . hal-02015899

HAL Id: hal-02015899

<https://hal.science/hal-02015899v1>

Submitted on 12 Feb 2019

HAL is a multi-disciplinary open access archive for the deposit and dissemination of scientific research documents, whether they are published or not. The documents may come from teaching and research institutions in France or abroad, or from public or private research centers.

L'archive ouverte pluridisciplinaire **HAL**, est destinée au dépôt et à la diffusion de documents scientifiques de niveau recherche, publiés ou non, émanant des établissements d'enseignement et de recherche français ou étrangers, des laboratoires publics ou privés.

1 Sampling of suspended particulate matter using particle traps in the
2 Rhône River: relevance and representativeness for the monitoring of
3 contaminants

4
5 Masson^{*}, M., Angot^a, H., Le Bescond, C., Launay, M., Dabrin, A., Miège, C., Le Coz, J.,
6 Coquery, M.

7
8 *Irstea, UR RiverLy, centre de Lyon-Villeurbanne, 5 rue de la Doua CS 20244, 69625 Villeurbanne,*
9 *France*

10 *a- Now at Institute for Data, Systems and Society, Massachusetts Institute of Technology, Cambridge,*
11 *MA, USA*

12
13 **Corresponding author: matthieu.masson@irstea.fr*

14
15 **Abstract**

16
17 Monitoring hydrophobic contaminants in surface freshwaters requires measuring contaminant
18 concentrations in the particulate fraction (sediment or suspended particulate matter, SPM) of the
19 water column. Particle traps (PTs) have been recently developed to sample SPM as cost-efficient,
20 easy to operate and time-integrative tools. But the representativeness of SPM collected with PTs is
21 not fully understood, notably in terms of grain size distribution and particulate organic carbon (POC)
22 content, which could both skew particulate contaminant concentrations. The aim of this study was to
23 evaluate the representativeness of SPM characteristics (i.e. grain size distribution and POC content)
24 and associated contaminants (i.e. polychlorinated biphenyls, PCBs; mercury, Hg) in samples collected

25 in a large river using PTs for differing hydrological conditions. Samples collected using PTs (n=74)
26 were compared with samples collected during the same time period by continuous flow
27 centrifugation (CFC).

28 The grain size distribution of PT samples shifted with increasing water discharge: the proportion of
29 very fine silts (2-6 μm) decreased while that of coarse silts (27-74 μm) increased. Regardless of water
30 discharge, POC contents were different likely due to integration by PT of high POC-content
31 phytoplankton blooms or low POC-content flood events. Differences in PCBs and Hg concentrations
32 were usually within the range of analytical uncertainties and could not be related to grain size or POC
33 content shifts. Occasional Hg-enriched inputs may have led to higher Hg concentrations in a few PT
34 samples (n = 4) which highlights the time-integrative capacity of the PTs. The differences of annual
35 Hg and PCB fluxes calculated either from PT samples or CFC samples were generally below 20%.
36 Despite some inherent limitations (e.g. grain size distribution bias), our findings suggest that PT
37 sampling is a valuable technique to assess reliable spatial and temporal trends of particulate
38 contaminants such as PCBs and Hg within a river monitoring network.

39

40 **Keywords:** hydrophobic contaminants, continuous flow centrifugation, grain size distribution,
41 particulate organic matter, particle trap, Rhône River

42 **1. Introduction**

43 The monitoring of contaminant concentrations and fluxes in surface waters is necessary for
44 assessing and managing environmental pollution in continental hydro-systems. Typical examples of
45 challenging regulations are the European Union Water Framework Directive (WFD) (European
46 Commission, 2000) which aims at achieving the good ecological and chemical status of European
47 water bodies, and the Barcelona Convention (UNEP, 1976) which encourages the contracting parties
48 to evaluate the pollution discharge delivered by watercourses to the Mediterranean Sea. As
49 hydrophobic and lipophilic substances tend to preferentially accumulate in suspended particulate
50 matter (SPM) rather than in the dissolved phase, SPM sampling is recommended as an alternative
51 method to water sampling for the monitoring of these contaminants in rivers (Lepom et al., 2009;
52 Schubert et al., 2012; Schulze et al., 2007). Suspended particulate matter sampling is preferred to
53 bed material sampling as particle deposition is often spatially heterogeneous and includes bed
54 materials.

55 Various sampling techniques can be used to collect SPM including direct water sampling (manual
56 grab sampling or use of automatic samplers) followed by filtration (Duinker et al., 1979; Mahler and
57 Van Metre, 2003) or settling (Etcheber and Jouanneau, 1980), in-line filtration (Horowitz, 1986),
58 continuous flow centrifugation (CFC; Burrus et al., 1989; Rees et al. 1991; Schäfer and Blanc, 2002) or
59 the deployment of particle traps (PT; Gardner, 1980; Phillips et al., 2000; Pohlert et al., 2011). Under
60 usual SPM concentrations in rivers ($1-100 \text{ mg L}^{-1}$ typically), direct water sampling requires collecting
61 too huge volumes of water, in order to provide enough material ($>2 \text{ g dry weight, d.w.}$) for the
62 analysis of a set of elements and contaminants including major parameters, metals, organic
63 contaminants and radioelements. The deployment of most SPM sampling methods in the field is
64 expensive, difficult, labor intensive and not always adequate. For instance, CFC requires permanent
65 technical attendance for several hours typically, which is difficult and costly to implement to
66 document the spatial and temporal trends of contamination throughout a large river network.
67 Furthermore, SPM sampling frequency (typically 4-6 samples per station and per year) is usually far

68 too low to record the high temporal variability of the hydrological regime with variable SPM sources
69 and contaminant concentrations (Schulze et al., 2007).

70 To overcome these problems, PTs are an alternative tool to sample SPM, since they are cost-
71 efficient, easy to operate and time-integrative (Phillips et al., 2000; Schulze et al., 2007). A PT can be
72 deployed regardless of SPM concentrations in the river, since the frequency at which the PT is
73 emptied can be adjusted. A monitoring network can thus be spatially and temporally extended using
74 PTs: more stations can be equipped for the same cost. Moreover, integrative-sampling over long
75 periods of time accounts for all flood events, during which the main part of the annual particulate
76 flux is transported. A standardized model of PT (Schulze et al., 2007) is already used to collect SPM
77 samples in rivers as part of the German Environmental Specimen Bank, to support the assessment of
78 long-term trends in contaminant concentrations (Koschorreck et al., 2015). Based on this technique,
79 retrospective studies of metals, arsenic (Fliedner et al., 2014), triclosan, methyl-triclosan residues
80 (Rüdel et al., 2013), polychlorobiphenyls (PCBs), and hexachlorobenzene (Schubert et al., 2012) in
81 SPM of different German rivers have recently been published.

82 Whereas the representativeness of SPM samples collected by CFC was investigated and validated
83 as early as 25 years ago (e.g. Burrus et al., 1989; Horowitz et al., 1989; Rees et al., 1991), the
84 representativeness of the particles collected with PTs is still questionable and not fully understood.
85 This question is arguably the main obstacle to a wider use of PTs in river pollution monitoring
86 programs. Some studies suggested that SPM sampled by PT may differ from SPM in the river, which
87 was reflected by a modification of SPM parameters such as grain size distribution (particle
88 fractionation effects) or organic carbon content (Allan et al., 2009; Ciffroy et al., 1999; Pohlert et al.,
89 2011; Schubert et al., 2012). This representativeness issue is a serious concern because it could lead
90 to biased concentrations for contaminants (e.g. Lacey et al., 2017) that usually have a strong affinity
91 for fine particles, due to an increasing specific area with decreasing grain size (Duinker, 1986; Olsen
92 et al., 1982; Pierard et al., 1996), or for organic rich particles (Karickhoff et al., 1979; Olsen et al.,
93 1982). Also, Russel et al. (2000) showed that the sediment collected by the PT described by Phillips et

94 al (2000) provided representative SPM samples of the river in terms of major elements (total carbon
95 and phosphorous) and metals (e.g. Fe, Mn, As, Pb, Zn) concentrations (with respect to the laboratory
96 analytical errors). Pohlert et al. (2011) reported a systematic study that intended to address the
97 representativeness of SPM samples collected with a PT, which unfortunately was also different in size
98 and design (different inlets/outlets, sloped bottom, no baffles) from the German standardized
99 model. Their study relied on SPM samples collected using this PT and two other systems, CFC and an
100 in-situ isokinetic sampler. Their results showed similar PCB concentrations in SPM collected by the
101 three systems, but differences in particle-size, organic carbon and hexachlorobenzene contents were
102 observed. The relative importance of particle segregation and time-integration effects could not be
103 clearly disentangled, since CFC samples are not time-integrative. Moreover, analytical uncertainties
104 of contaminant concentrations were not reported and their potential contributions in the differences
105 observed between sampling techniques were not considered.

106 Since 2009, within the Rhône Sediment Observatory (OSR) program, PTs designed according to
107 the German PT described by Schulze et al. (2007) have been routinely used for the monitoring of
108 particulate contaminants throughout the Rhône River (from Lake Geneva to the Mediterranean Sea).
109 The objective of this study was to determine the physico-chemical representativeness of SPM
110 samples collected by PT in a large river under various hydrological conditions, i.e. under a wide range
111 of flow velocities and SPM concentrations. To fulfil this objective, we compared physico-chemical
112 characteristics of SPM collected using both PT and CFC (reference sampling method) over a period of
113 four years. The particle fractionation effects were investigated using an original method based on the
114 deconvolution of the grain size distributions. Additionally, POC, PCBs and Hg concentrations were
115 analyzed and analytical uncertainties evaluated, to assess the potential bias in particulate
116 concentrations induced by the sampling method. To allow an efficient comparison of data obtained
117 by integrative (PT) and punctual (CFC) sampling techniques, time-integration effects were considered
118 in this study based on SPM fluxes during PT deployment.

119

120 **2. Material and Methods**

121 **2.1 Sampling strategy**

122 The comparison of SPM sampling methods was based on SPM samples collected within the OSR
123 program by both PT (n=74) and CFC (n=85) in the Rhône River at Jons, France (Fig. 1). The location of
124 this sampling station is strategic as it integrates the upper part of the Rhône River watershed
125 (~20000 km²) upstream of the Lyon urban area. Grain size distribution or POC content of SPM may
126 differ depending on hydrological conditions (Allan et al., 2009; Ciffroy et al., 1999; Pohlert et al.,
127 2011; Schubert et al. 2012). Therefore, this study covered a long period of time (August 2012 - July
128 2016) characterized by base flow periods (discharge < 800 m³ s⁻¹) and several flood events (discharge
129 > 800 m³ s⁻¹).

130 Since no hydrometric station exists at Jons, daily discharges at this station were computed using a
131 1-D hydrodynamical model (Dugué et al., 2015) from the discharge inputs of the Rhône River, the
132 Bourbre River and the Ain River (Fig. 1). At the Jons station, mean daily SPM concentrations were
133 computed from in situ turbidity measurements every 15 min using a Hach Lange SC200 turbidity
134 probe, with turbidity-SPM concentration curves calibrated using frequent water sampling and
135 filtration.

136 The duration of the PT deployments in the river was 2 weeks generally, in order to collect a
137 sufficient amount of SPM for physico-chemical analysis (> 2 g d.w.). To compare SPM collected by PT
138 with those collected by CFC (reference sampling method), each deployment of PT was systematically
139 bordered with two SPM samplings by CFC carried out during the PT installation and recovery days.
140 The recovery of a trap is normally followed by the re-installation of the emptied trap; the sampling of
141 SPM by centrifugation is systematically carried out just beforehand.

142

143 **2.2 SPM recovery and treatment**

144 The PTs used in this study and in the OSR monitoring network were built identical to PTs
145 described in Schulze et al. (2007). They consist of a high quality (type 316 L) stainless steel box with

146 three holes on the front and back faces allowing water circulation inside (Fig. 2). Two baffles induce a
147 decrease of the current velocity within the PT, firstly by overflow and secondly by underflow,
148 allowing the decantation of SPM into two sedimentation tanks. At the Jons station, the PT was
149 immersed on the river bank at ~4-5 m above the bottom at a cross-section with well-mixed
150 suspension, with fairly homogeneous SPM concentrations (Launay, 2014). Particles trapped in the
151 two tanks were collected and mixed together in the largest tank using a clean Teflon spatula, then
152 conditioned in an amber glass bottle (for chemical analysis) and in a polypropylene (PP) tube (for
153 grain size determination).

154 Sampling using CFC was achieved with a stationary CEPA Z61 high speed centrifuge or a mobile
155 Westfalia KA-2 centrifuge. Water was directly pumped from the Rhône River (50-100 cm below the
156 water surface) to the centrifuge with a flow of ~700-800 L h⁻¹. The end of the pumping pipe was
157 installed approximately 5 m downstream of the PT in order to avoid issues related to the possible
158 non-homogeneity of SPM throughout the river cross-section. During base flow periods,
159 approximately 3000 L of river water were sampled, while during floods, lower water volumes were
160 adjusted (depending on the turbidity) in order to collect more than 2 g (d.w.) of particles. After
161 centrifugation, particles deposited on a Teflon sheet (for the stationary CFC) or in a Teflonated bowl
162 (for the mobile CFC) were collected for the same analyses as the PT samples.

163 Suspended particulate matter collected in the glass bottles were deep-frozen and freeze-dried as
164 soon as brought to the laboratory. The freeze-dried samples were grinded and homogenized with an
165 agate ball mill (PM200, Retsch), then stored in the dark in dry atmosphere until chemical analysis.
166 Suspended particulate matters collected in PP tubes were stored at 4°C in the dark until grain size
167 distribution analysis.

168

169 **2.3 Analytical methods**

170 Volumetric grain size distribution of SPM was assessed by laser diffraction using a Cilas 1190
171 particle size analyzer according to the ISO 13320 standard method (AFNOR, 2009). A representative

172 wet sub-sample was introduced into the analyzer respecting good obscuration rate (typically 15%).
173 The volumetric grain size distribution of the sample was computed using the Fraunhofer optical
174 model (AFNOR, 2009).

175 The determination of POC in SPM samples collected before December 2014 was performed using
176 a carbon analyzer (Thermo Electron, CHN Flash 2000) by INRA laboratory (Arras, France).
177 Decarbonation was completed using hydrochloric acid according to the NF ISO 10694 standard
178 method (AFNOR, 1995). The limit of quantification (LOQ) was estimated to be 0.05 g kg^{-1} and
179 analytical uncertainty varied between $\sim 3\%$ and $\sim 6\%$ ($k=2$), depending on the POC concentration. For
180 samples collected after December 2014, POC analyses were conducted by Irstea laboratory using a
181 similar carbon analyzer (Thermo Electron, CN Flash 2000) and a method adapted from the NF ISO
182 10694 standard method (AFNOR, 1995) and manufacturer recommendation. The LOQ was estimated
183 to be 0.5 g kg^{-1} . A reference material from a proficiency interlaboratory testing (Aglae, 15M9.1;
184 40 g kg^{-1}) was systematically used to control analytical accuracy (93%) and uncertainty (8%; $k=2$).

185 The determination of total Hg in SPM was performed using an automated atomic absorption
186 spectrophotometer, DMA 80 (Milestone), according to EPA method 7473 (EPA, 2007). The LOQ of Hg
187 in SPM was $10 \mu\text{g kg}^{-1}$. Blanks and certified reference materials (IAEA 433, marine sediment; LGC
188 6187, river sediment) were systematically used to control analytical accuracy (94%) and uncertainty
189 (14%; $k=2$).

190 The contents of the so-called indicator PCBs (congeners 28, 52, 101, 118, 138, 153, and 180) were
191 analyzed in SPM according to the French Standard XP X33-012 (AFNOR, 2000). Approximately 1.0 g
192 (d.w.) of sample was extracted with a cyclohexane/acetone 90:10 v/v mixture, concentrated by
193 evaporation and purified on a 1 g Florisil SPE cartridge. A small amount of copper powder was finally
194 added in order to avoid sulfur interferences prior to gas chromatography analysis with a ^{63}Ni
195 electron capture detector (GC-ECD). Samples were analyzed on two different columns (RTX[®]-5,
196 $30 \text{ m} \times 0.25 \text{ mm} \times 0.25 \mu\text{m}$ and RTX[®]-PCB, $30 \text{ m} \times 0.25 \text{ mm} \times 0.25 \mu\text{m}$) to confirm the results. The
197 accuracy of measurements was checked via intercomparison exercises and the analysis of a

198 reference material (BCR 536). A sample of sediment from the Bourbre River, a tributary of the Rhône
199 River, was used to determine analytical uncertainties, as no certified reference material exists for
200 such low levels of PCBs in equivalent matrix. The LOQs were estimated between 0.5 and 2.5 $\mu\text{g kg}^{-1}$
201 depending on the current analytical conditions (e.g. condition of the radioactive beta particle
202 emitter) and on the congeners. Analytical uncertainties were estimated to be 60% ($k=2$) for
203 concentrations lower than 3-times the LOQ and to be 30% ($k=2$) for concentrations higher than 3-
204 times the LOQ.

205

206 **2.4 Data treatment and statistical analysis**

207 *2.4.1 Grain size distribution*

208 The grain size distribution of SPM collected in the Rhône River is multimodal, as is the case in
209 most rivers of this size (Launay, 2014). As a consequence, the traditional summary of grain size
210 distribution by some percentile diameters (e.g., d_{50} , d_{10} , d_{90}) may not be representative of the
211 dominant particle populations in the samples. The particle size distribution of a homogeneous
212 population of SPM is generally regarded as a lognormal distribution due to the sorting process
213 applied to the particles during their transport in the stream (e.g. Blott and Pye 2001). The mixture of
214 different homogeneous sub-populations is expected to yield a mixture of Gaussian distributions for
215 the logarithms of diameters, which can be identified in measured grain size distributions using a
216 calibration procedure (Launay, 2014). The normalmixEM function included in the R Package Mixtools
217 (Benaglia et al., 2009) was applied to identify the parameters of the mixture of normally distributed
218 populations. The calculation is done iteratively by the method of maximum likelihood with the
219 Expectation Maximization algorithm suggested by Dempster et al. (1977). The user provides the
220 population to be studied and the number of Gaussian distributions to be identified in the combined
221 probability density function. For the studied SPM samples, between 2 and 4 (3 in most cases)
222 gaussian laws were generally observed. The normalmixEM function returns i) the mode (μ ; in μm), ii)
223 the standard deviation (σ ; in μm), and iii) the proportion (λ ; in %), of each fitted Gaussian distribution

224 (Fig. 3). A Gaussian distribution was discarded as spurious in case any of the following conditions was
225 not met: $\mu < 1 \mu\text{m}$, $\sigma > 0.5 \mu\text{m}$ or $\lambda < 1\%$.

226

227 2.4.2 Statistical tests

228 Statistical tests were used for data comparison and correlation determination. For each test, a
229 preliminary study of the data was performed to determine whether the data sets were normally
230 distributed (using Shapiro-Wilk test) with equal variances. As all the data sets tested do not meet
231 these conditions, non-parametric tests were used: Wilcoxon test (two-tailed) for the comparison of
232 mean values and Kendall test for correlation determination. A summary of each statistical test
233 (conditions and results) is presented in Table 1 with conclusions given on the basis of a significance
234 level of 0.05.

235

236 2.4.2 Temporal comparison of PT and CFC sampling

237 The evaluation of the representativeness of SPM collected by PT was performed by the
238 comparison of the physico-chemical parameters (grain size distribution, POC) and contaminants (Hg,
239 PCBs) with those measured on SPM collected by CFC (reference samples). To allow an accurate
240 comparison of the concentrations measured in SPM collected by an integrative sampler (PT) and by
241 punctual sampling (CFC), and thus reduce the time-integration effects, a mean concentration of each
242 parameter i ($C_{ref,i}$) was calculated from the two CFC samples bordering a PT period (i.e. the
243 corresponding reference samples). To take into account the variation of SPM concentration during
244 the PT deployment, $C_{ref,i}$ was calculated as the mean concentration of the parameter i measured in
245 the two CFC samples ($C_{start,i}$ at the installation and $C_{end,i}$ at the recovery of the PT) weighted by the
246 SPM masses (m_1 and m_2) transported at the sampling site during each half-period of PT deployment:

$$247 \quad C_{ref,i} = \frac{m_1 \times C_{start,i} + m_2 \times C_{end,i}}{m_1 + m_2} \quad (1)$$

248 The SPM masses m_1 and m_2 were computed from hourly discharges and hourly SPM concentrations
249 during each half-period of PT deployment. The relative error (in %) was calculated to compare the
250 concentration of a parameter i obtained after PT sampling ($C_{PT,i}$) with its reference concentration
251 ($C_{ref,i}$):

$$252 \text{ relative } i \text{ error} = \frac{C_{PT,i} - C_{ref,i}}{C_{ref,i}} \quad (2)$$

253 A statistical approach was used to determine any significant difference among the concentrations
254 of physico-chemical parameters in SPM sampled by PT and CFC. For each parameter, the difference
255 between $C_{PT,i}$ and $C_{ref,i}$ was compared with the analytical uncertainty expressed as one standard
256 deviation (which corresponds to the 68% confidence interval for a Gaussian distribution),
257 respectively $s_{PT,i}$ and $s_{ref,i}$ (estimated using error propagation approach from Eq. 1 and taking a
258 precision on the estimation of SPM fluxes estimated to be 20%; Launay, 2014). In this way, the
259 difference of concentrations measured between SPM sampled by PT and CFC may be included in the
260 analytical uncertainties if the following equation is verified:

$$261 |C_{PT,i} - C_{ref,i}| \leq 1.96 \sqrt{s_{PT,i}^2 + s_{ref,i}^2} \quad (3)$$

262 Therefore, this approach includes both the analytical uncertainties and time integration effect of PT.

263

264 2.4.3 Estimation of contaminant fluxes

265 Mercury and PCB 138 fluxes were estimated at the annual scale using mean hourly discharges and
266 mean hourly SPM concentrations in order to estimate hourly SPM fluxes. In case of SPM
267 concentration gaps, hourly SPM concentrations were estimated from a robust relationship between
268 discharge and SPM concentrations obtained at the Jons station (Poulier et al., submitted to this
269 issue). Hourly contaminant fluxes were calculated by multiplying hourly SPM fluxes by hourly
270 contaminant concentrations estimated either from PT samples (the Hg or PCB concentration

271 measured in a PT sample was applied throughout the deployment period at the hourly scale) or from
272 CFC samples (the Hg or PCB concentration measured in a CFC were applied on both sides of the two
273 half periods of PT deployments). In case of Hg or PCB concentration gaps, contaminant
274 concentrations were set depending on hydrological conditions (base flow or flood periods) (Poulier et
275 al., submitted to this issue). All PCB concentrations below the LOQ were replaced by the LOQ value.
276 Hourly contaminant fluxes were finally summed up over the period of interest.

277

278 **3. Results**

279 **3.1 Water discharge and SPM concentrations**

280 During the studied period (August 2012 to July 2016), the daily water discharge varied from 181 to
281 $2147 \text{ m}^3 \text{ s}^{-1}$ (Fig. 4a). Generally, wet seasons with several floods occurred during late fall, winter and
282 spring (November-April), and a dry period was observed during summer and early fall (August-
283 October). In contrast, the discharge remained exceptionally low from May 2015 to December 2016
284 with only one short flood event, and important flood events were recorded during summer 2014.
285 Suspended particulate matter concentration was highly variable, ranging from $<2 \text{ mg L}^{-1}$ (i.e. $<\text{LOQ}$)
286 to 668 mg L^{-1} (Fig. 4b), in relation with the discharge variations. The comparison of SPM
287 concentration during the different periods (i.e. PT deployment period and the two days of CFC
288 sampling) was achieved through the discharge-weighted average SPM concentration (SPM_{wa}), i.e.
289 calculated as the ratio of the SPM flux to the water flux estimated during the corresponding periods
290 (deployment period for PT and the day of the CFC was achieved). The SPM_{wa} concentration varied
291 from $<2 \text{ mg L}^{-1}$ to 285 mg L^{-1} during PT deployment periods (S.I.1) and from $<2 \text{ mg L}^{-1}$ to 500 mg L^{-1} for
292 SPM sampling by CFC (S.I.2).

293

294 **3.2 Grain size distribution**

295 The grain size distribution of SPM collected by PT ranged from ~ 0.1 to $400 \mu\text{m}$ (e.g. Fig. 3a) and
296 was composed of three sub-populations of particles (i.e. three Gaussian modes were observed;

297 Fig. 5). For SPM collected by CFC, the grain size distribution ranged from ~ 0.1 to $112 \mu\text{m}$ (Fig. 3b).
298 Three modes were also observed in two-thirds of the samples but only two modes were observed in
299 the remaining samples (Fig. 5). All these modes may be classified in three classes (Fig. 5),
300 corresponding to very fine silts for the finest mode (median diameters, μ_1 , ranging from 2.0 to
301 $6.0 \mu\text{m}$), medium silts for the intermediate mode (median diameters, μ_2 , ranging from 9.4 to
302 $20.7 \mu\text{m}$) and very coarse silts for the coarser mode (median diameters, μ_3 , ranging from 27.3 to
303 $74.1 \mu\text{m}$), according to the classification of Friedman and Sanders (1978). While the mean
304 proportions of the medium silts (λ_2) were similar for SPM collected by PT ($55 \pm 9\%$) and CFC ($52 \pm$
305 12%) (Wilcoxon test #1, Table 1), significant differences were observed for the finest (λ_1) and
306 coarsest (λ_3) modes (Wilcoxon test #2 and #3, Table 1): on average, the PT samples contained -20%
307 of very fine silts and +16% of very coarse silts than those collected by CFC (Fig. 5). Additionally, the
308 mean diameters of the 2nd and 3rd modes (μ_2 and μ_3) were coarser for the PT samples ($16.4 \mu\text{m}$ and
309 $48.6 \mu\text{m}$, respectively) than for the CFC samples ($12.7 \mu\text{m}$ and $35.2 \mu\text{m}$, respectively). These results,
310 and the absence of the 3rd mode in one third of SPM samples collected by CFC, demonstrate that
311 SPM sampled by the PT were clearly coarser than those sampled by the CFC.

312 To simplify the description of the grain size distributions, proportions obtained for the finest two
313 modes were added ($\lambda_1 + \lambda_2$). These proportions varied between 53% and 97% for the PT samples and
314 between 78% and 100% for the CFC samples (Fig. 4c, S.I.3) with mean values significantly different
315 (Wilcoxon test #4, Table 1). The proportions of fine particles were clearly lower for the PT samples
316 than for the CFC samples as suggested by the box plots (Fig. 4c).

317

318 **3.3 Chemical composition**

319 Particulate organic carbon concentrations measured in SPM collected by the PT varied between
320 14 and 50 g kg^{-1} and those measured in the CFC samples varied between 12 and 70 g kg^{-1} (Fig. 4d;
321 S.I.3). The mean POC concentrations measured in PT (26 g kg^{-1}) and CFC samples (29 g kg^{-1}) were not
322 significantly different (Wilcoxon test #5, Table 1) as shown by the box plots. These concentrations are

323 well within the range of values observed in the downstream part of the Rhône River: 30-60 g kg⁻¹
324 (Cauwet et al., 1990) and 8-27 g kg⁻¹ (Cathalot et al., 2013).

325 Mercury concentrations measured in SPM collected by PT and CFC varied from 0.029 to
326 0.190 mg kg⁻¹ and from 0.034 to 0.112 mg kg⁻¹, respectively (Fig. 4e; S.I.3). Mean Hg concentrations
327 measured in PT (0.056 ± 0.023 mg kg⁻¹) and CFC samples (0.057 ± 0.015 mg kg⁻¹) were not
328 significantly different (Wilcoxon test #6, Table 1) as shown by the box plots. Except for one PT
329 sample, these values were below the threshold effect concentration (TEC; 0.18 mg kg⁻¹) that should
330 not be exceeded to avoid negative effects on aquatic wildlife (MacDonald et al., 2000). Mean Hg
331 concentrations were close to the average Hg concentration observed in the upper continental crust
332 (i.e. 0.056 mg kg⁻¹; Wedepohl, 1995).

333 The concentrations of PCBs were measured in 80% of the collected samples (S.I.4 and 5).
334 Concentrations of PCB 28 and PCB 52 measured in SPM collected by PT and CFC were almost always
335 below the LOQ (less than 5% of quantified values; S.I.3). The congener 118 was quantified in 30% and
336 37% of samples collected by PT and CFC, respectively. The percentages of quantified values for the
337 four other congeners (101, 138, 153 and 180) were higher and varied from 69% to 88% (S.I.3). The
338 minimum PCB concentration measured in SPM was <0.5 µg kg⁻¹ (lowest LOQ) for all congeners (S.I.3).
339 The maximum PCB concentration measured in SPM was higher for the four PCB congeners with the
340 highest quantification frequency (congeners 101, 138, 153 and 180; between 3.14 and 5.16 µg kg⁻¹)
341 than for the others (congeners 28, 52 and 118; between 0.54 and 2.13 µg kg⁻¹). The sum of the seven
342 indicator PCBs (for values lower than the LOQs, concentrations equal to the LOQs were used) ranged
343 between 4.0 and 18.2 µg kg⁻¹ and did not exceed the TEC value (59.8 µg kg⁻¹; MacDonald et al., 2000).
344 These concentrations are similar to those measured in sediments of the Rhône River sampled
345 upstream of the Lyon agglomeration from mid-1990s to 2010 which are still considered as
346 contaminated, despite a decrease in concentrations since 1980s (Desmet et al., 2012). Strong
347 correlations were found between the four PCB congeners (data below LOQ were excluded) with the
348 highest quantification frequency, i.e. PCB 101, PCB 138, PCB 153 and PCB 180 (Kendall test #7,

349 Table 1; Table 2). This suggests that these 4 congeners have a similar behavior in SPM, even if the
350 concentrations of PCB 101 and 180 are lower than those of PCB 138 and 153 (S.I.3). For this reason,
351 we decided to simplify the study by focusing on PCB 138 thereafter, as this congener was well
352 quantified in SPM and has one of the best correlation factors with the other congeners. The mean
353 PCB 138 concentrations measured in CFC ($1.95 \pm 0.78 \mu\text{g kg}^{-1}$) and PT samples ($2.31 \pm 0.79 \mu\text{g kg}^{-1}$)
354 were not significantly different (Wilcoxon test #8, Table 1) as suggested by the box plots (Fig. 4f) and
355 similar median values (less than 5% difference; S.I.3).

356

357 **4. Discussion**

358 **4.1 Representativeness of the grain size distribution of SPM sampled by PT**

359 The grain size distributions of SPM collected by CFC during base flow and flood periods were
360 similar (Fig. 5) as confirmed by statistical tests (Wilcoxon test #9, Table 1) carried out on the coarser
361 particle class proportions (λ_3). For SPM collected by PT, very coarse silts prevailed during flood
362 periods (Wilcoxon test #10, Table 1) with a mean proportion of 34% vs. 19% during base flow
363 periods. Consequently, the differences between SPM sampled by PT and CFC seem to be amplified
364 during flood periods. The relative error of fine particle proportion ($\lambda_1 + \lambda_2$) in PT samples (vs. CFC)
365 varied between -4% and -44% (S.I.1) with mean values significantly different (Wilcoxon test #11,
366 Table 1) between base flow periods (-15%) and flood periods (-29%). Moreover, a strong negative
367 relationship was observed between the relative fine particle proportion ($\lambda_1 + \lambda_2$) error (see Eq. 2)
368 and the mean discharge during PT deployment periods (Fig. 6). Thus, the grain size distribution of
369 SPM sampled by PT was highly dependent on hydrological conditions. This phenomenon has already
370 been reported by Phillips et al. 2000 who showed that SPM trapped in the Phillips PT became
371 significantly coarser than SPM of the water flow when the current velocity reached $0.6 \text{ m}\cdot\text{s}^{-1}$. It is
372 however unclear whether the PT induced a loss of finest particles and/or a gain of coarsest particles.
373 The potential loss of finest particles by PT has already been reported in several studies (Phillips et al.,
374 2000; Pohlert et al., 2011; Schubert et al., 2012). Schäfer and Blanc (2002) also suggested that an

375 increase of flow energy induced a decrease of the trapping efficiency for fine particles that do not
376 enter in the PT. The present study clearly shows that all particles sizes were captured by PT, including
377 the smallest ones: the properties of the sub-populations were conserved; however their proportions
378 may differ as a function of flow velocity. A better understanding of how this PT works should be
379 provided by future hydraulic flume experiments based on protocols reported by Phillips et al. (2000)
380 or Smith and Owens (2014), for example.

381

382 **4.2 Representativeness of the chemical composition of SPM sampled by PT**

383 *4.2.1 Organic Matter*

384 Particulate organic carbon concentration decreased with increasing SPM_{wa} concentration (Fig. 7a)
385 to reach values between 10 and 20 g kg⁻¹ (Kendall test #12, Table 1). Similar trends are generally
386 observed in surface waters (e.g. Paolini, 1995; Veyssy et al., 1998) and may be explained by a dilution
387 of autochthonous particulate organic matter (e.g. phytoplankton) by less-enriched organic land-
388 derived material during flood periods (Meybeck, 1982). This is supported by the range of total
389 organic concentrations (4 and 8 g kg⁻¹) measured in the subsoil of the region of interest (Salminen et
390 al., 2005).

391 The relative error of POC concentrations in PT samples (vs. CFC) varied between -56% and +57%,
392 except one outlier reaching +98% during base flow. No correlation was observed between relative
393 POC error and SPM_{wa} concentration (Fig. 7b), which suggests that the origin (i.e. autochthonous or
394 land-derived material) of particulate organic matter does not explain the differences in POC
395 concentrations measured in SPM sampled by PT and CFC. Furthermore, no correlation was observed
396 between relative POC error and the relative fine particle proportion ($\lambda_1 + \lambda_2$) error (Fig. 7c). The
397 general coarsening of grain size distribution of SPM sampled by PT is unlikely to influence POC
398 concentration directly. Therefore, POC was probably distributed evenly among the three main classes
399 of particles composing the grain size distribution of SPM sampled in the Rhône River at the Jons
400 station. This hypothesis is reinforced by the results of an experiment in which similar POC

401 concentrations were measured in sub-fractions of SPM samples fractionated as a function of particle
402 size (granulometric sorting according to gravity; Launay, 2014). Moreover, excluding the most
403 extreme value (98%), relative POC errors were normally distributed around 2% (Shapiro–Wilk
404 test #13, Table 1). The presented results do not support the hypothesis of a loss of fine-particulate
405 matter and light organic material with the overflow as proposed by Schubert et al. (2012).

406 Alternatively, the degradation of rapidly biodegradable organic matter in the PT during the
407 sampling period could influence SPM quality (Schubert et al., 2012). Figure 7d shows the relative POC
408 error as a function of time: alternating episodes with positive (i.e. over-estimation of POC by the PT)
409 and negative (i.e. under-estimation of POC by the PT) errors can be observed. From July 2012 to June
410 2014, positive POC errors were observed during summer and early fall, while negative values were
411 observed during winter and spring (Fig. 7d). This trend was not clearly observed thereafter.
412 Variations of relative POC errors may be due to a balance between two processes inside the PT: (i)
413 degradation of the organic matter trapped during the PT deployment period (Pohlert et al., 2011),
414 and (ii) production of organic matter such as bacterial growth. However, the fact that seasonal
415 variations were not systematically observed along years suggests that other phenomena should
416 contribute to the differences of POC concentrations between PT and CFC samples. In particular, PT
417 may integrate variations of organic matter quality such as phytoplankton blooms characterized by an
418 increase of POC concentrations, or flood events characterized by a decrease of POC concentrations
419 as mentioned above.

420

421 *4.2.2 Particulate mercury*

422 Mercury concentration increased with POC concentration in SPM samples collected by PT and CFC
423 (Fig. 8a; Kendall test #14, Table 1). This trend is due to the well-known strong affinity of Hg for
424 organic matter (e.g. Mason and Sullivan, 1998). Hence, Hg is also affected by the dilution of POC by
425 less-enriched organic land-derived material during flood periods. This is supported by the decrease of
426 Hg concentration with increasing SPM concentration (Fig. 8b). The mean Hg concentrations (S.I.3) of

427 the PT and CFC samples during flood periods, i.e. 0.047 and 0.051 mg kg⁻¹, respectively, were
428 significantly different (Wilcoxon test #15 and #16, Table 1) from the mean concentrations measured
429 during base flow periods, i.e. 0.056 and 0.057 mg kg⁻¹, respectively. During flood periods and for
430 *SPM_{wa}* concentrations above 100 mg L⁻¹, Hg concentrations of PT and CFC samples (n=10) tend
431 toward 0.03-0.05 mg kg⁻¹ (Fig. 8b); these concentrations correspond to the Hg geochemical
432 background level estimated between 0.03 and 0.04 mg kg⁻¹ from soil samples in this region (Salminen
433 et al., 2005). This suggests that SPM carried during the flood periods at the Jons station were not Hg-
434 enriched. In contrast, increases of particulate Hg concentrations were measured during floods in the
435 Lower Rhône at the Arles station (in November 2008). This could be attributed to Cevenol Rivers that
436 drain Hg rich-areas (Launay, 2014).

437 The relative error of Hg concentration in PT samples (vs. CFC) varied from -52% to +42% (Fig. 8c),
438 except for five values between +69% and +154% that correspond to PT samples with the highest Hg
439 concentrations. No correlation was observed between the relative Hg and POC errors (Fig. 8c)
440 despite the correlation observed between COP and Hg concentrations. This suggests that the
441 potential changes in POC concentration inside the PT did not directly affect Hg concentration. Bias-
442 correction attempts of Hg concentration measured in the PT by relative POC error were unsuccessful
443 as they did not allow the reduction of the relative Hg errors. Other hypotheses may explain
444 differences between Hg concentration measured in SPM sampled by PT and CFC:

445 (1) Variation of grain size distribution: coarse particles generally support lower levels of metals
446 and organic contaminants (e.g. Klamer et al., 1990). However, the variations in grain size
447 distributions, which are coarser for the PT samples than for the CFC samples, especially during flood
448 periods, do not seem to contribute to the relative Hg errors (Fig. 8d). Again, bias-correction attempts
449 of the Hg concentrations measured in the PT by grain size distribution (for example by the finest
450 particle proportion errors) were unsuccessful.

451 (2) Time-integration effects of the PT may be important if Hg concentration of SPM changes over
452 time. This for instance occurred between April, 23rd and May, 6th 2013: a flood was recorded on the

453 Bourbre River on April, 27th. The Bourbre River is known to have high Hg concentrations in SPM,
454 generally exceeding 0.100 mg kg^{-1} (Thollet et al., 2015). This flood event is the reason why Hg
455 concentration measured in SPM sampled at the Jons station using PT (0.107 mg kg^{-1}) was higher than
456 Hg concentration measured in the two corresponding CFC samples (0.042 and 0.044 mg kg^{-1} ; Fig. 4e).
457 In the same vein, a substantial contribution of the Bourbre River to the SPM flux at the Jons station
458 from the 14th to 28th of August 2012 (Dabrin et al., submitted to this issue) may explain the high Hg
459 concentration measured in the PT sample at Jons (0.107 mg kg^{-1}) and the high relative Hg error of
460 82%.

461 (3) The analytical uncertainties may be another explanation as they are 2-4 times greater for Hg
462 analysis (14%) than for POC analysis (3-8%). Larger analytical uncertainties may add noise to the
463 relative Hg errors and may explain the absence of correlation between relative Hg errors and POC
464 errors. It is therefore critical to account for analytical uncertainties when comparing Hg
465 concentrations between PT and CFC samples (see section 4.3)

466

467 4.2.2 PCB 138

468 Unlike Hg concentration, no clear correlation was observed between PCB 138 and POC
469 concentrations (Fig. 8f). This suggests that particulate organic matter was not the main carrier phase
470 of PCB 138 in the Upper Rhône River. During periods with the highest SPM_{wa} concentrations (typically
471 $>100 \text{ mg L}^{-1}$), PCB 138 concentrations tend towards low values (0.67 - $1.35 \text{ } \mu\text{g kg}^{-1}$; Fig. 8g) as observed
472 for Hg. This may indicate that resuspension of bed and bank materials by floods induced input of less
473 contaminated sediments. Moreover, the main sources of PCBs to the Rhône River are reported to be
474 located downstream of the sampling station, in Lyon urban area and some tributaries of the Lower
475 Rhône River (Mourier et al., 2014).

476 The relative error of PCB 138 concentration in PT samples (vs. CFC) was estimated only if the
477 concentrations measured in the PT and the two corresponding CFC samples were above the LOQ
478 (50% of the situations; $n=35$). The relative PCB 138 error varied from -45% to +60% (Fig. 8h), except

479 for three PT samples (between +123% and +161%) which were sampled during a limited period, from
480 November 2012 to February 2013. These 3 samples were different from the 5 PT samples with the
481 highest Hg error values, suggesting that potential Hg and PCB sources are different. The relative
482 PCB 138 errors were related neither to relative POC errors (Fig. 8h) nor to fine particle proportion
483 errors (Fig. 8i).

484

485 **4.3 Accounting for analytical uncertainties in the comparison**

486 In this study, the concentrations of contaminants measured in SPM sampled by PT and CFC were
487 compared with consideration of analytical uncertainties, which had not been the case in most other
488 studies (e.g. Pohlert et al., 2011; Shubert et al., 2012). Russel et al. (2000) indicated that the
489 differences of metals (such as As, Pb, Zn) concentrations between SPM samples collected by PT
490 (Philipps device) and manually were generally below analytical uncertainties. The comparison of
491 absolute contaminant concentrations with their analytical uncertainties (see Eq. 3) allowed
492 determining if there was any significant difference among the concentrations of contaminants in
493 SPM sampled by PT and CFC. For Hg, 51 pairs of samples (PT and CFC) out of 70 in total (i.e. 73%) had
494 Hg concentrations that were not significantly different with respect to the analytical uncertainties
495 (Fig. 8e). This proportion was higher during base flow periods (80%) than during flood periods (53%).
496 For PCB 138, 31 pairs of out of 35 (i.e. 89%) had PCB concentrations that were not significantly
497 different with respect to the analytical uncertainties (Fig. 8j). This proportion was greater than those
498 observed for Hg and may be partly explained by a higher analytical uncertainty for PCB 138 (30-60%
499 depending on the concentration; $k=2$) than Hg (14%; $k=2$). As for Hg, the proportion of sample pairs
500 for which the difference in PCB 138 concentration can be explained by the analytical uncertainties
501 was higher during base flow periods (96%) than during flood periods (67%).

502 During base flow periods, most of Hg and PCB 138 concentrations measured in PT samples are
503 comparable with those measured in CFC samples when analytical uncertainties are taken into
504 account. However, some differences, not fully attributable to analytical uncertainties, were observed

505 mostly during flood periods. Moreover, we observed the absence of correlation between relative
506 contaminant (Hg or PCB 138) errors and SPM characteristics (POC or fine particle proportion) errors.
507 These results suggest that the differences in Hg and PCB 138 (and other PCB congeners, by
508 extension) between PT and CFC samples concentrations are due to integrative effect of the PT. In
509 other words, the differences of contaminants observed between PT and CFC samples are attributed
510 to: i) analytical uncertainties (whose effect was estimated), ii) differences in terms of grain size and
511 POC contents (whose effects seemed negligible), and iii) the integrative capacity of the PT (whose
512 effects were demonstrated during specific hydrological events). This emphasizes the capacity of SPM
513 sampling by PT to integrate the whole peak of Hg and PCB concentrations, which may be limited in
514 duration and thus easily missed by punctual sampling by CFC.

515

516 **4.4 Relevance of PT sampling to assess annual SPM and contaminant fluxes**

517 One of the main objectives of OSR program is the estimation of annual contaminant fluxes
518 transported with SPM along the river. Annual Hg and PCB 138 fluxes at Jons station were estimated
519 from Hg and PCB 138 concentrations measured in either PT or CFC samples for 2013, 2014 and 2015
520 (Table 3). Annual Hg fluxes varied between 25.8 and 38.5 kg y⁻¹ for PT data and between 30.2 and
521 42.5 kg y⁻¹ for CFC data. Annual PCB 138 fluxes varied between 1.25 and 2.16 kg y⁻¹ for PT data and
522 between 0.94 and 1.79 kg y⁻¹ for CFC data. The differences of annual Hg and PCB 138 fluxes
523 estimated using PT or CFC data were below 20% (Table 3), except for PCB 138 fluxes in 2015 where
524 the difference reached 48% (mainly due to PCB 138 concentrations below the LOQ measured in three
525 CFC samples during flood periods in April and May, while concentrations measured in the PT samples
526 were close to 3 µg kg⁻¹; Fig. 4f). Again, this result highlights the advantage of the integrative capacity
527 of PTs for the monitoring of contaminants in SPM.

528 Mercury and PCB fluxes were also estimated for two distinct periods of about 7 to 8 months
529 (periods chosen to avoid as many gaps as possible) with contrasted hydrological regimes: the first
530 period (from 9th April to 22th October 2013) is characterized by 3 flood events; the second period

531 (from 7th May to 22th December 2015) may be described as a dry period with low discharge. For these
532 two periods, the differences of Hg and PCB fluxes estimated from PT and CFC data were below 20%
533 (between 3% and 18%; Table 3).

534 These results demonstrate that cumulated contaminant fluxes estimated from either PT or CFC
535 samples are similar at the annual scale. This is due to i) the good agreement between Hg/PCB 138
536 concentrations measured in SPM sampled by PT and CFC, with relative Hg and PCB 138 errors
537 generally centered around the null value, and especially to ii) the low range of variation of
538 contaminant concentrations compared to that of discharge and SPM concentrations (Fig. 4a, e and f).
539 Therefore, we conclude that PT can be considered as a reliable SPM sampling technique for the long-
540 term monitoring of Hg and PCB cumulated fluxes in rivers at the annual or multi-month scale. In fact,
541 annual budgets of SPM and associated contaminants (Hg and PCBs) in the Rhône River have recently
542 been estimated using contaminant concentrations measured in PT samples (Poulier et al., submitted
543 to this issue).

544

545 **5. Conclusion**

546 The relevance and representativeness of SPM collected in rivers with PT were studied with
547 consideration of i) the integrative effect of PT compared to CFC, the latter being assimilated to
548 punctual sampling, and ii) the analytical uncertainties. The comparison of physical and chemical
549 characteristics of SPM collected by PT and CFC allowed drawing the following conclusions:

550 i) A deconvolution method of grain size distributions into Gaussian distributed sub-populations
551 showed that SPM sampled in the Rhône River at the Jons station consisted of a mixture of three
552 classes of particles: very fine silts, medium silts and very coarse silts. The grain size distribution was
553 coarser in PT than in CFC samples. However, all classes of particles were captured by PT with a shift –
554 highly dependent on water discharge – from very fine silts towards coarser silts.

555 ii) Particulate organic carbon concentrations measured in the PT and CFC samples depended on
556 the origin of SPM: less-enriched organic land-derived material (mainly during flood periods) or

557 autochthonous more-enriched material (mainly during base flow periods). The relative errors (from -
558 52% to +42%) of POC concentrations in PT samples vs. CFC cannot be attributed to differences in
559 grain size distribution. Instead, integration of events such as phytoplankton blooms or floods by the
560 PT contributed to an increase or a decrease, respectively, of POC concentrations in the PT samples
561 compared to the CFC samples. Hypothetical variations of POC concentrations by production and/or
562 degradation of organic matter inside the PT during its deployment remain to be demonstrated.

563 iii) Mercury concentrations measured in PT and CFC samples were correlated with POC
564 concentrations and thus affected by hydrological conditions. The relative errors for Hg concentration
565 (between -52% to +42%, typically) were acceptable and can be explained by analytical uncertainties.
566 The highest relative Hg errors were related to the highest Hg concentrations measured in PT samples
567 and were explained by the punctual contribution of a Hg-enriched tributary during the PT
568 deployment period.

569 iv) Only 4 out of the 7 indicator PCBs (congeners 101, 138, 153 and 180) were quantified in more
570 than 50% of the PT and CFC samples. These congeners showed a similar behavior: an increase in
571 grain size or a POC shift did not influence their concentrations in the PT samples. The relative errors
572 for PCB concentrations (typically from -45% to +60%) were acceptable. For the vast majority (89%) of
573 samples, the relative error was in the range of analytical uncertainties. Outliers, mainly observed
574 during flood periods, were attributed to the time integration effect of PT sampling.

575 Despite the grain size distribution bias towards coarser particles and/or potential organic matter
576 production/degradation, PTs can be considered as a reliable tool for SPM sampling within the aim of
577 Hg and PCBs concentration/flux monitoring. It is however important that PTs are well positioned in
578 the river flow, i.e. a few meters above river-bottom and in a cross-section with homogeneous SPM
579 concentrations. As i) all classes of particles are captured and ii) grain size distribution of SPM is
580 relatively fine (mainly silts), the concentrations of contaminants other than those studied in this
581 work, such as polycyclic aromatic hydrocarbons, should be similar, with respect to analytical
582 uncertainties, whether they are measured in SPM collected using PT or CFC techniques. A future

583 study on the effect of particle size distribution bias on metal concentrations is planned using another
584 field SPM data. Furthermore, this study highlighted the main advantage of SPM sampling by PTs:
585 samples are time integrative and are thus representative of SPM and associated contaminants
586 transported in the river during periods of time with varying hydrological conditions. Future
587 experiments in controlled tilting flume are planned to improve our understanding of sampling
588 processes within PT and possibly reduce grain size distribution bias through modification of PT shape.

589

590

591 **Acknowledgments**

592 This study was supported by the Rhône Sediment Observatory (OSR), a multi-partner research
593 program partly funded by the *Plan Rhône* and by the European Regional Development Fund (ERDF)
594 allocated by the European Union. We gratefully acknowledge the following Irstea colleagues for SPM
595 sampling, field campaigns, sample treatment, chemical analysis and data analysis: Myriam Arhror,
596 Marie Courtel, Guillaume Dramais, Ghislaine Grisot, Mickaël Lagouy, Josselin Panay, Benjamin
597 Renard, Loïc Richard and Fabien Thollet.

598

599

600 **References**

601

602 AFNOR, 2009. NF ISO 10694: Particle size analysis - Laser diffraction methods. 51 pp.

603 AFNOR, 2000. XP X33-012: Characterisation of sludges - Determination of polynuclear aromatic hydrocarbons
604 (PAH) and polychlorinated biphenyls (PCB). 28 pp.

605 AFNOR, 1995. NF ISO 10694: Soil quality - Determination of organic and total carbon after dry combustion
606 (elementary analysis). 7 pp.

- 607 Allan, I., Fjeld, E., Garmo, Ø., Langford, K., Kringstad, A., Bratsberg, E., Kaste, Ø., 2009. RiverPOP: Measuring
608 concentrations of persistent organic pollutants and trace metals in Norwegian rivers. SFT-report TA
609 2521/2009, NIVA-sno 5815, 112 pp.
- 610 Benaglia, T., Chauveau, D., Hunter, D.R., Young, D.S., 2009. Mixtools: an R package for analyzing finite mixture
611 models. *J. Stat. Softw.* 32, 1-29.
- 612 Blott, S.J., Pye, K., 2001. GRADISTAT: A grain size distribution and statistics package for the analysis of
613 unconsolidated sediments. *Earth Surf. Processes Landforms* 26, 1237-1248.
- 614 Burrus, D., Thomas, R.L., Dominik, J., Vernet, J.P., 1989. Recovery and concentration of suspended-solids in the
615 upper Rhone river by continuous-flow centrifugation. *Hydrol. Processes* 3, 65-74.
- 616 Cathalot, C., Rabouille, C., Tisnerat-Laborde, N., Toussaint, F., Kerherve, P., Buscail, R., Loftis, K., Sun, M.Y.,
617 Tronczynski, J., Azoury, S., Lansard, B., Treignier, C., Pastor, L., Tesi, T., 2013. The fate of river organic carbon
618 in coastal areas: A study in the Rhone River delta using multiple isotopic (δ C-13, δ C-14) and organic
619 tracers. *Geochim. Cosmochim. Acta* 118, 33-55.
- 620 Cauwet, G., Gadel, F., Sierra, M.M.D., Donard, O., Ewald, M., 1990. Contribution of the Rhone river to organic-
621 carbon inputs to the northwestern mediterranean-sea. *Cont. Shelf Res.* 10, 1025-1037.
- 622 Ciffroy, P., Vazelle, D., Mataix, V., Taconnet, J., Estèbe, A., Thévenot, D., Bourguignon, O., Idlafkih, Z., Meybeck,
623 M., 1999. Comparison of methods for sampling suspended matter in rivers: application to measurement of
624 particulate metals. *Hydroécologie Appliquée* 11, 71-102.
- 625 Dabrin, A., Bretier, M., Dugué, V., Masson, M., Le Bescond, C., Le Coz, J., Coquery, M., submitted. Reactivity of
626 particulate element concentrations: assessment of suspended particulate matter sources in the Rhône
627 River, France. Submitted to *Sci. Total Environ.*, this issue.
- 628 Dempster, A., Laird, N., Rubin, D., 1977. Maximum likelihood from incomplete data via EM algorithm. *J. Roy.*
629 *Stat. Soc. B Met.* 39, 1-38.
- 630 Desmet, M., Mourier, B., Mahler, B.J., Van Metre, P.C., Roux, G., Persat, H., Lefèvre, I., Peretti, A., Chapron, E.,
631 Simonneau, A., Miège, C., Babut, M., 2012. Spatial and temporal trends in PCBs in sediment along the lower
632 Rhône River, France. *Sci. Total Environ.* 433, 189-197.
- 633 Dugué, V., Walter, C., Andries, E., Launay, M., Le Coz, J., Camenen, B., Faure, J.B., 2015. Accounting for
634 hydropower schemes' rules in the 1-D hydrodynamic modeling of the Rhône River from Lake Geneva to the
635 Mediterranean sea. 36th IAHR World Congress, 28 June - 3 July 2015, The Hague, the Netherlands.

- 636 Duinker, J.C., 1986. The role of small, low-density particles on the partition of selected PCB congeners between
637 water and suspended matter (North-Sea area). *Neth. J. Sea Res.* 20, 229-238.
- 638 Duinker, J.C., Noltin, R.F., Vandersloot, H.A., 1979. The determination of suspended metals in coastal waters by
639 different sampling and processing techniques (filtration, centrifugation). *Neth. J. Sea Res.* 13, 282-297.
- 640 EPA, 2007. Method 7473: Mercury in solids and solutions by thermal decomposition, amalgamation, and
641 atomic absorption spectrophotometry. 17 pp.
- 642 Etcheber, H., Jouanneau, J.M., 1980. Comparison of the different methods for the recovery of suspended
643 matter from estuarine waters: Deposition, filtration and centrifugation; Consequences for the
644 determination of some heavy metals. *Estuar. Coast. Shelf Sci.* 11, 701-707.
- 645 European Commission, 2000. Directive 2000/60/EC of the European Parliament and of the Council of 23
646 October 2000 establishing a framework for Community action in the field of water policy. *Off. J. Eur.*
647 *Commun.* L327.
- 648 Fliedner, A., Rudel, H., Knopf, B., Weinfurtner, K., Paulus, M., Ricking, M., Koschorreck, J., 2014. Spatial and
649 temporal trends of metals and arsenic in German freshwater compartments. *Environ. Sci. Pollut. Res.* 21,
650 5521-5536.
- 651 Friedman, G.M., Sanders, F.E., 1978. *Principles of sedimentology*, Wiley, New York.
- 652 Gardner, W.D., 1980. Field assessment of sediment traps. *J. Mar. Res.* 38, 41-52.
- 653 Horowitz, A.J., 1986. Comparison of methods for the concentration of suspended sediment in river water for
654 subsequent chemical analysis. *Environ. Science Technol.* 20, 155-160.
- 655 Horowitz, A.J., Elrick, K.A., Hooper, R.C., 1989. A comparison of instrumental dewatering methods for the
656 separation and concentration of suspended sediment for subsequent trace-element analysis. *Hydrol.*
657 *Processes* 3, 163-184.
- 658 Karickhoff, S.W., Brown, D.S., Scott, T.A., 1979. Sorption of hydrophobic pollutants on natural sediments. *Water*
659 *Res.* 13, 241-248.
- 660 Klamer, J.C., Hegeman, W.J.M., Smedes, F., 1990. Comparison of grain size correction procedures for organic
661 micropollutants and heavy metals in marine sediments. *Hydrobiologia* 208, 213-220.
- 662 Koschorreck, J., Heiss, C., Wellmitz, J., Fliedner, A., Rudel, H., 2015. The use of monitoring data in EU chemicals
663 management-experiences and considerations from the German environmental specimen bank. *Environ. Sci.*
664 *Pollut. Res.* 22, 1597-1611.

- 665 Lacey, J.P., Evrard, O., Smith, H.G., Blake, W.H., Olley, J.M., Minella, J.P.G., Owens, P.N., 2017. The challenges
666 and opportunities of addressing particle size effects in sediment source fingerprinting: A review. *Earth-Sci.*
667 *Rev.* 169, 85-103.
- 668 Launay, M., 2014. Fluxes of suspended particulate matters, particulate mercury and PCBs in the Rhône River
669 from lake Geneva to the Mediterranean Sea. PhD Thesis (in French), University of Lyon, 432 pp.
- 670 Lepom, P., Brown, B., Hanke, G., Loos, R., Quevauviller, P., Wollgast, J., 2009. Needs for reliable analytical
671 methods for monitoring chemical pollutants in surface water under the European Water Framework
672 Directive. *J. Chromatogr. A* 1216, 302-315.
- 673 MacDonald, D.D., Ingersoll, C.G., Berger, T.A., 2000. Development and evaluation of consensus-based sediment
674 quality guidelines for freshwater ecosystems. *Arch. Environ. Contam. Toxicol.* 39, 20-31.
- 675 Mahler, B.J., Van Metre P.C., 2003. A simplified approach for monitoring hydrophobic organic contaminants
676 associated with suspended sediment: Methodology and applications. *Arch. Environ. Contam. Toxicol.* 44,
677 288-297.
- 678 Mason, R.P., Sullivan, K.A., 1998. Mercury and methylmercury transport through an urban watershed. *Wat.*
679 *Res.* 32, 321-330.
- 680 Meybeck, M., 1982. Carbon, nitrogen, and phosphorus transport by world rivers. *Am. J. Sci.* 282, 401-450.
- 681 Mourier, B., Desmet, M., Van Metre, P.C., Mahler, B.J., Perrodin, Y., Roux, G., Bedell, J.-P., Lefèvre, I., Babut, M.,
682 2014) Historical records, sources, and spatial trends of PCBs along the Rhone River (France). *Sci. Total*
683 *Environ.* 476-477, 568-576.
- 684 Olsen, C.R., Cutshall, N.H., Larsen, I.L., 1982. Pollutant particle associations and dynamics in coastal marine
685 environments - a review. *Mar. Chem.* 11, 501-533.
- 686 OSPAR, 2012. Levels and trends in marine contaminants and their biological effects – CEMP Assessment report
687 2012. 29 pp.
- 688 Paolini, J., 1995. Particulate organic-carbon and nitrogen in the Orinoco River (Venezuela). *Biogeochemistry* 29,
689 59-70.
- 690 Phillips, J.M., Russell, M.A., Walling, D.E., 2000. Time-integrated sampling of fluvial suspended sediment: a
691 simple methodology for small catchments. *Hydrol. Process.* 14, 2589-2602.
- 692 Pierard, C., Budzinski, H., Garrigues, P., 1996. Grain-size distribution of polychlorobiphenyls in coastal
693 sediments. *Environ. Science Technol.* 30, 2776-2783.

- 694 Pohlert, T., Hillebrand, G., Breitung, V., 2011. Effects of sampling techniques on physical parameters and
695 concentrations of selected persistent organic pollutants in suspended matter. *J. Environ. Monit.* 13, 1579-
696 1588.
- 697 Poulter, G., Launay, M., Le Bescond, C., Thollet, F., Coquery, M., Le Coz, J., submitted. Combining flux
698 monitoring and estimation to establish annual budgets of suspended particulate matter and associated
699 pollutants in the Rhône River from Lake Geneva to the Mediterranean Sea. Submitted to *Sci. Total Environ.*,
700 this issue.
- 701 Rees, T.F., Leenheer, J.A., Ranville, J.F., 1991. Use of a single-bowl continuous-flow centrifuge for dewatering
702 suspended sediments - effect on sediment physical and chemical characteristics. *Hydrol. Processes* 5, 201-
703 214.
- 704 Rüdell, H., Böhmer, W., Müller, M., Fliedner, A., Ricking, M., Teubner, D., Schröter-Kermani, C., 2013.
705 Retrospective study of triclosan and methyl-triclosan residues in fish and suspended particulate matter:
706 Results from the German Environmental Specimen Bank. *Chemosphere* 91, 1517-1524.
- 707 Russell, M.A., Walling, D.E., Hodgkinson, R.A., 2000. Appraisal of a simple sampling device for collecting time-
708 integrated fluvial suspended sediment samples. In: *The Role of Erosion and Sediment Transport in Nutrient*
709 *and Contaminant Transfer*. IAHS Press, Wallingford, UK, IAHS Publ. No. 263, pp. 119-127.
- 710 Salminen, R., Batista, M.J., Bidovec, M., et al., 2005. *Geochemical Atlas of Europe. Part 1 – Background*
711 *Information, Methodology and maps*. Geological Survey of Finland.
- 712 Schäfer, J., Blanc, G., 2002. Relationship between ore deposits in river catchments and geochemistry of
713 suspended particulate matter from six rivers in southwest France. *Sci. Total Environ.* 298, 103-118.
- 714 Schubert, B., Heininger, P., Keller, M., Ricking, M., Claus, E., 2012. Monitoring of contaminants in suspended
715 particulate matter as an alternative to sediments. *Trends Anal. Chem.* 36, 58-70.
- 716 Schulze, T., Ricking, M., Schroter-Kermani, C., Korner, A., Denner, H.D., Weinfurtner, K., Winkler, A., Pekdeger,
717 A., 2007. The German Environmental Specimen Bank - Sampling, processing, and archiving sediment and
718 suspended particulate matter. *J. Soils Sediments* 7, 361-367.
- 719 Smith, T.B., Owens, P.N., 2014. Flume- and field-based evaluation of a time-integrated suspended sediment
720 sampler for the analysis of sediment properties. *Earth Surf. Process. Landf.* 39, 1197-1207.
- 721 [dataset] Thollet F., Le Bescond C., Le Coz J., Coquery M., Panay J., Lagouy M., Dramais G., 2015. Observatoire
722 des Sédiments du Rhône, Irstea. <https://doi.org/10.17180/OBS.OSR>

- 723 UNEP, 1976. The 1976 Barcelona Convention for the Protection of the Mediterranean Sea Against Pollution.
724 United Nations Environment Programme (UNEP), 22 pp.
- 725 Veyssy, E., Etcheber, H., Lin, R.G., Buat-Menard, P., Maneux, E., 1998. Seasonal variation and origin of
726 Particulate Organic Carbon in the lower Garonne river at La Reole (southwestern France). *Hydrobiologia*
727 391, 113-126.
- 728 Wedepohl, K.H., 1995. The composition of the continental-crust. *Geochim. Cosmochim. Acta* 59, 1217-1232.

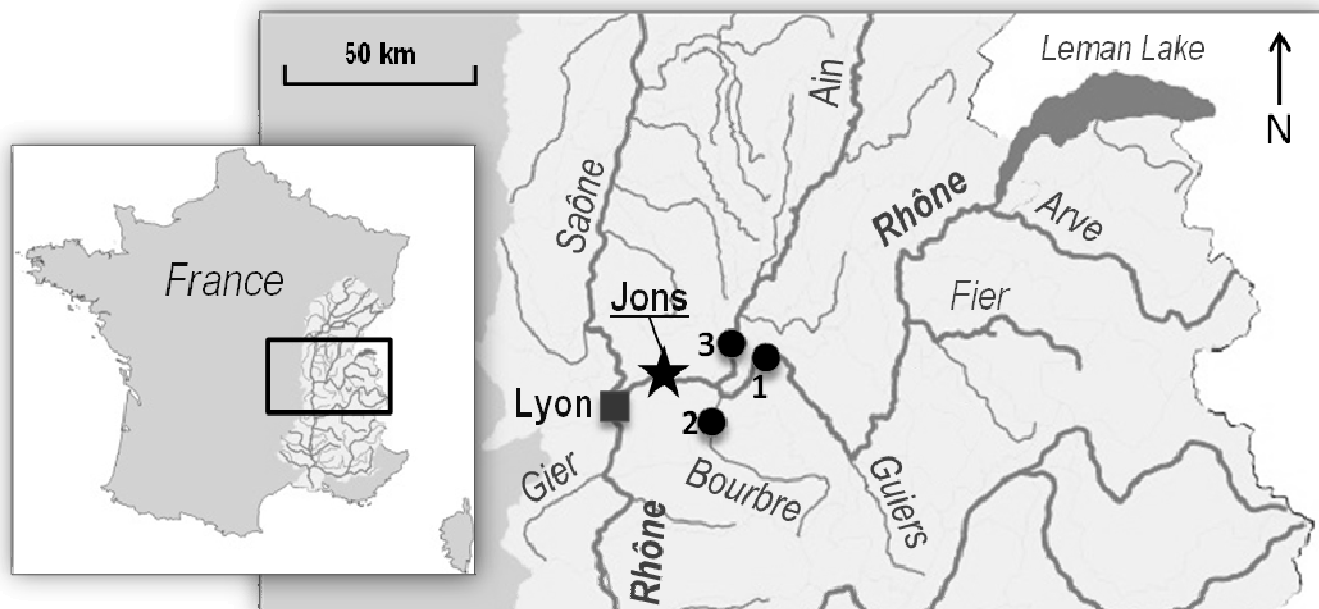


Figure 1: Map of the Upper course of the French Rhône River: SPM sampling at Jons station (black star) and river discharge measurements stations (solid circles) at 1. Lagnieu (Rhône River); 2. Tignieu-Jameyzieu (Bourbre River); 3. Chazey (Ain River); (discharge stations operated by CNR “Compagnie Nationale du Rhône”).

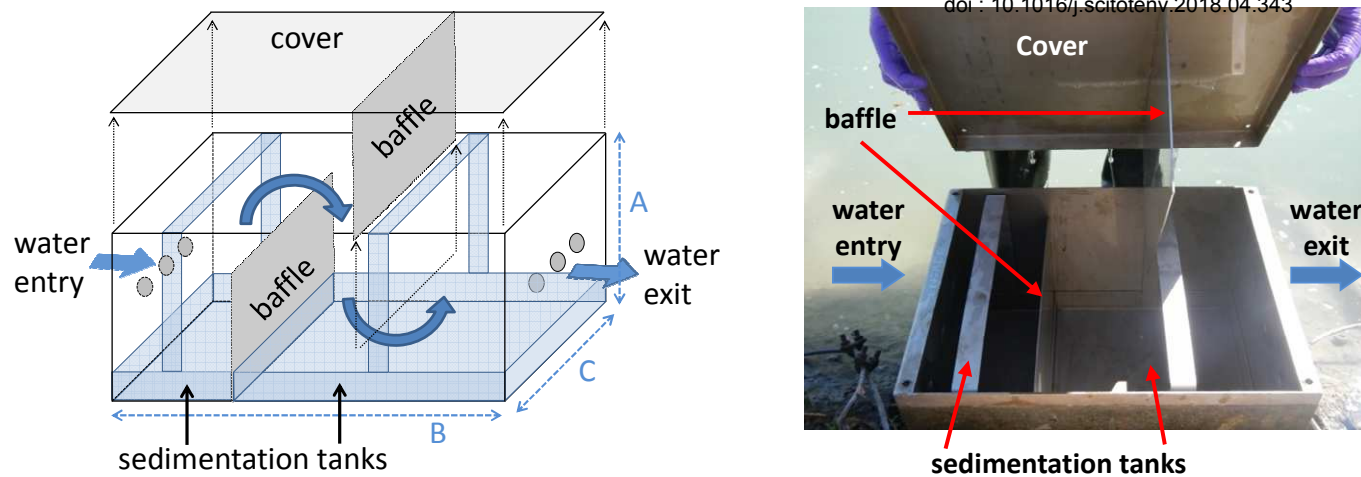


Figure 2: Scheme and picture of the particle trap (PT) used to collect SPM; A=250 mm, B=400 mm, C=300 mm.

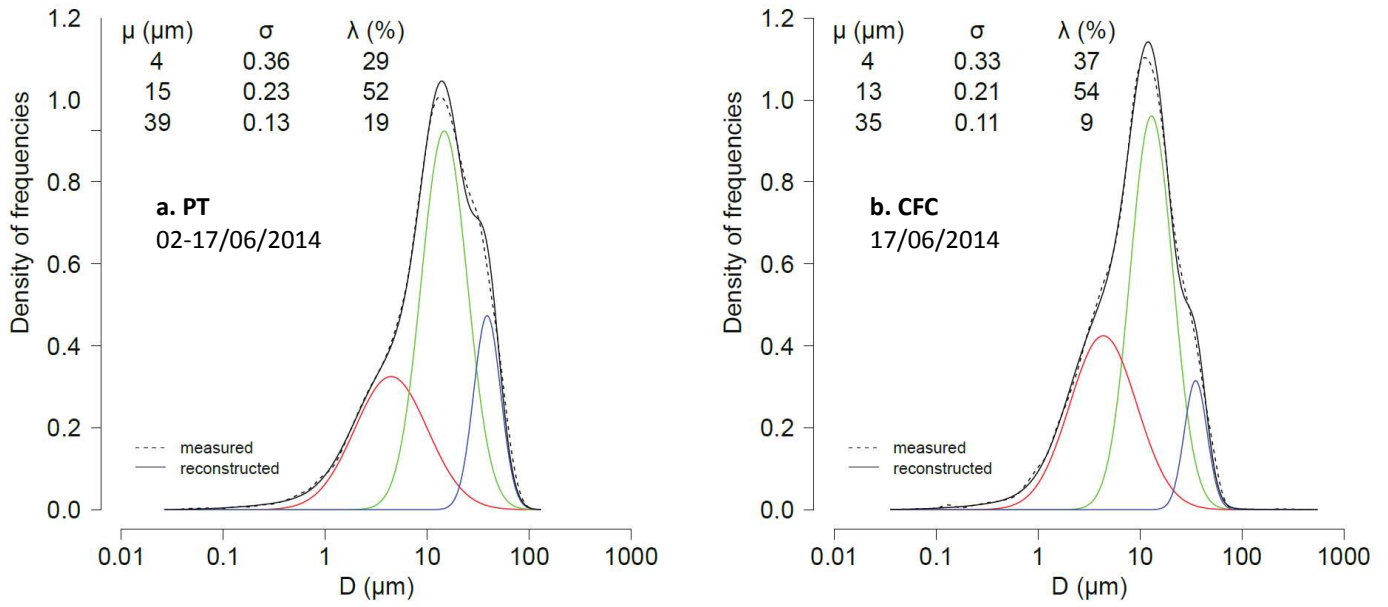


Figure 3: Examples of decomposition in three Gaussian distributions (red, green and blue lines) of the volumetric grain-size distribution (dashed line) of SPM samples collected at Jons station by (a) PT and (b) CFC techniques. The black solid line is the sum of the 3 Gaussian distributions.

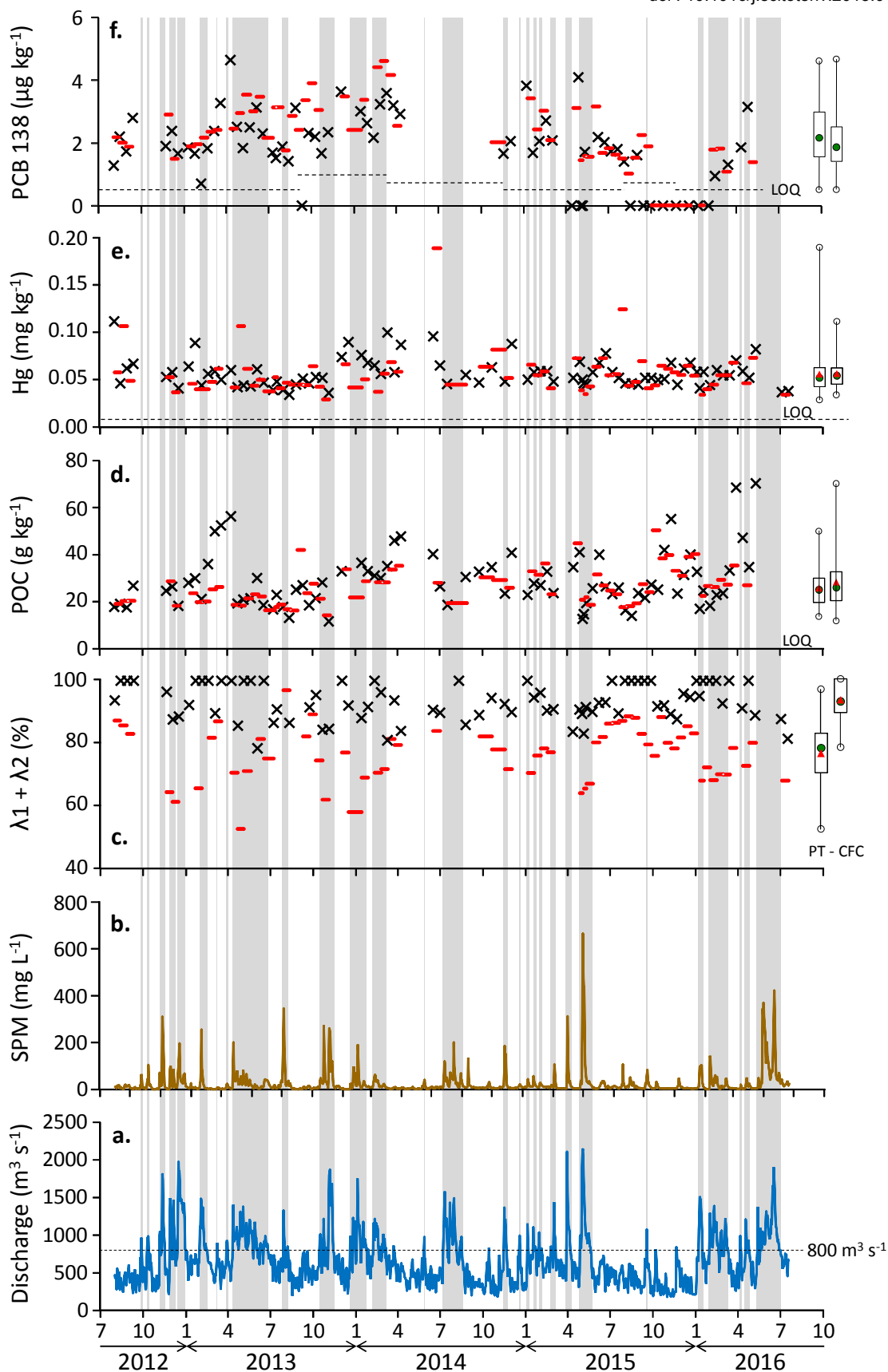


Figure 4: Parameters measured at Jons station from August 2012 to July 2016 (x-axis : years and months expressed in numbers): (a) hourly water discharges, (b) SPM concentrations, (c) proportions of the finest particles (sum of λ_1 and λ_2), (d) POC, (e) Hg and (f) PCB138 concentrations measured in SPM samples collected by CFC (black crosses) and PT (red). The dashed lines represent the LOQ for Hg and PCB138. Symbols on the x-axis represent samples with concentrations below the LOQ. The box plots for PT values (left) and CFC values (right) represent minimum and maximum (black circles), 1st and 3rd quartiles (box), mean (red triangle) and median (green circle) concentrations. Grey areas represent the flood periods (daily water discharge $>800 \text{ m}^3 \text{ s}^{-1}$).

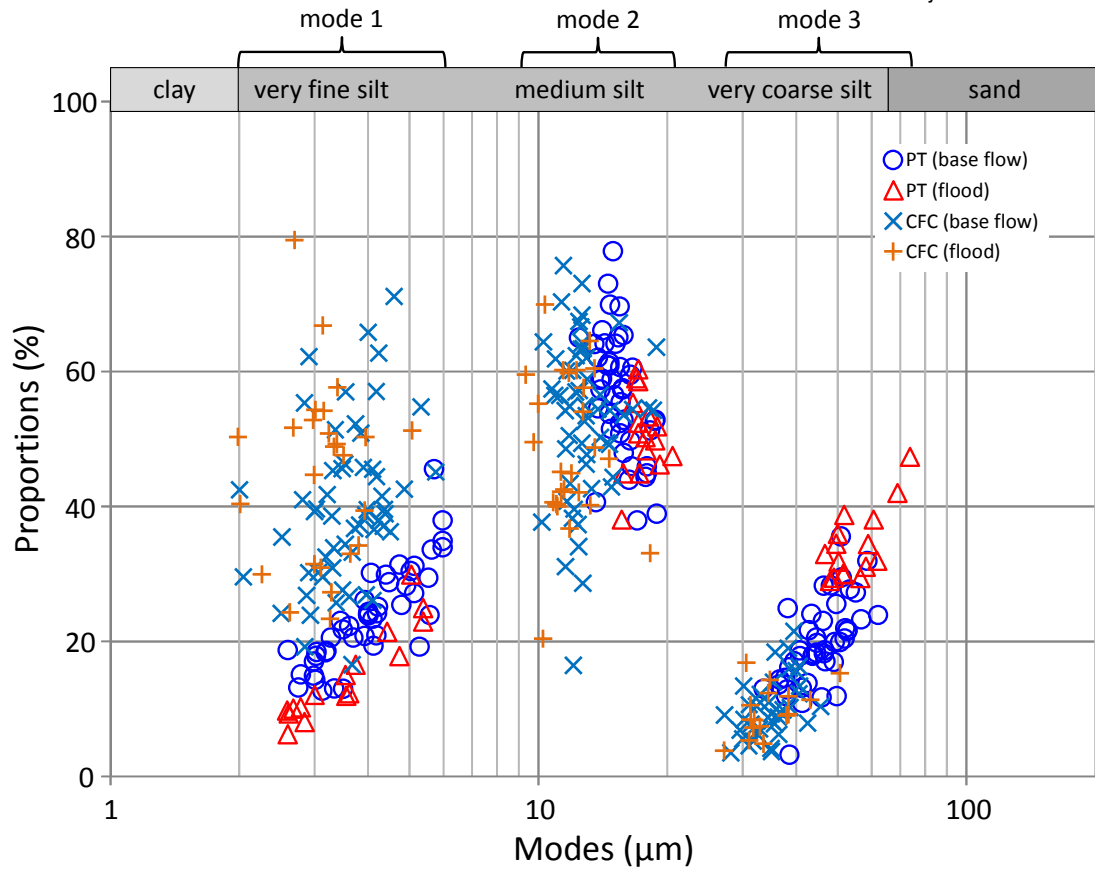


Figure 5: Modes and associated proportions of the Gaussian populations extracted for the grain size distributions of SPM sampled at the Jons station by PT and CFC for base flow and flood periods.

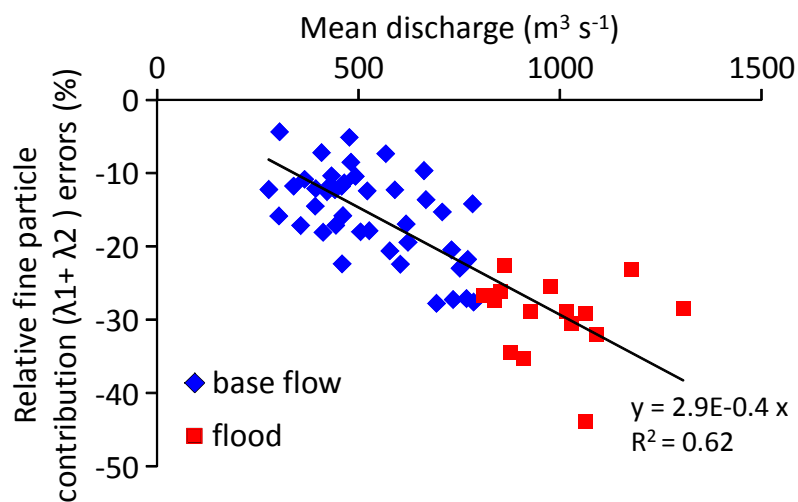


Figure 6: Relative errors of the fine particle proportions (expressed as the sum of the proportion of the two finest modes λ_1 and λ_2) as a function of the mean water discharge calculated during the PT deployment period at the Jons station from August 2012 to July 2016.

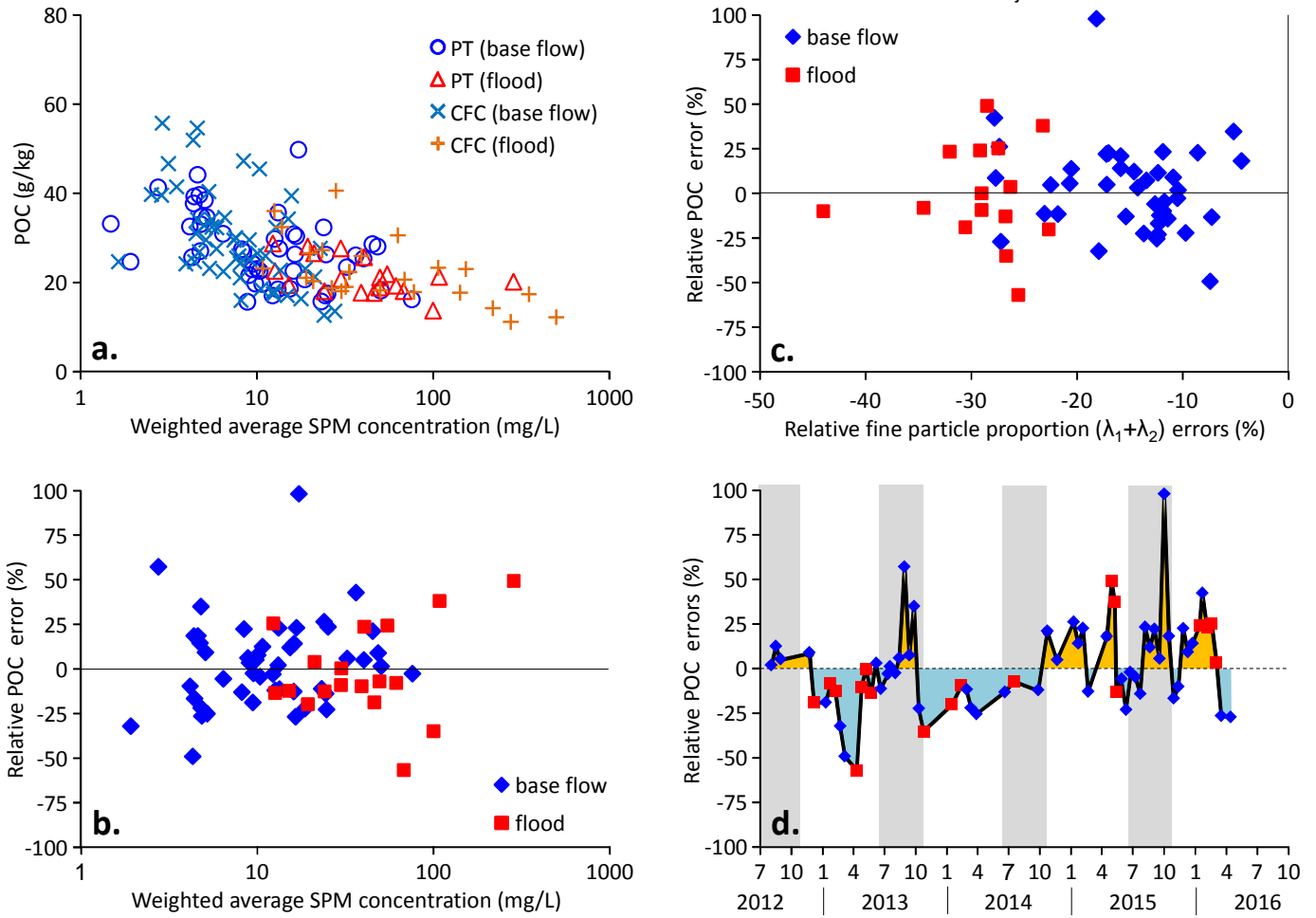


Figure 7: Trends in the POC concentrations measured in SPM samples collected by PT and CFC techniques at the Jons station from August 2012 to July 2016: (a) POC concentrations vs. weighted average SPM concentrations; (b) relative POC errors vs. weighted average SPM concentrations; (c) relative POC errors vs. relative fine particle proportion ($\lambda_1 + \lambda_2$) errors; (d) relative POC errors vs. time (grey areas show summer and early fall periods).

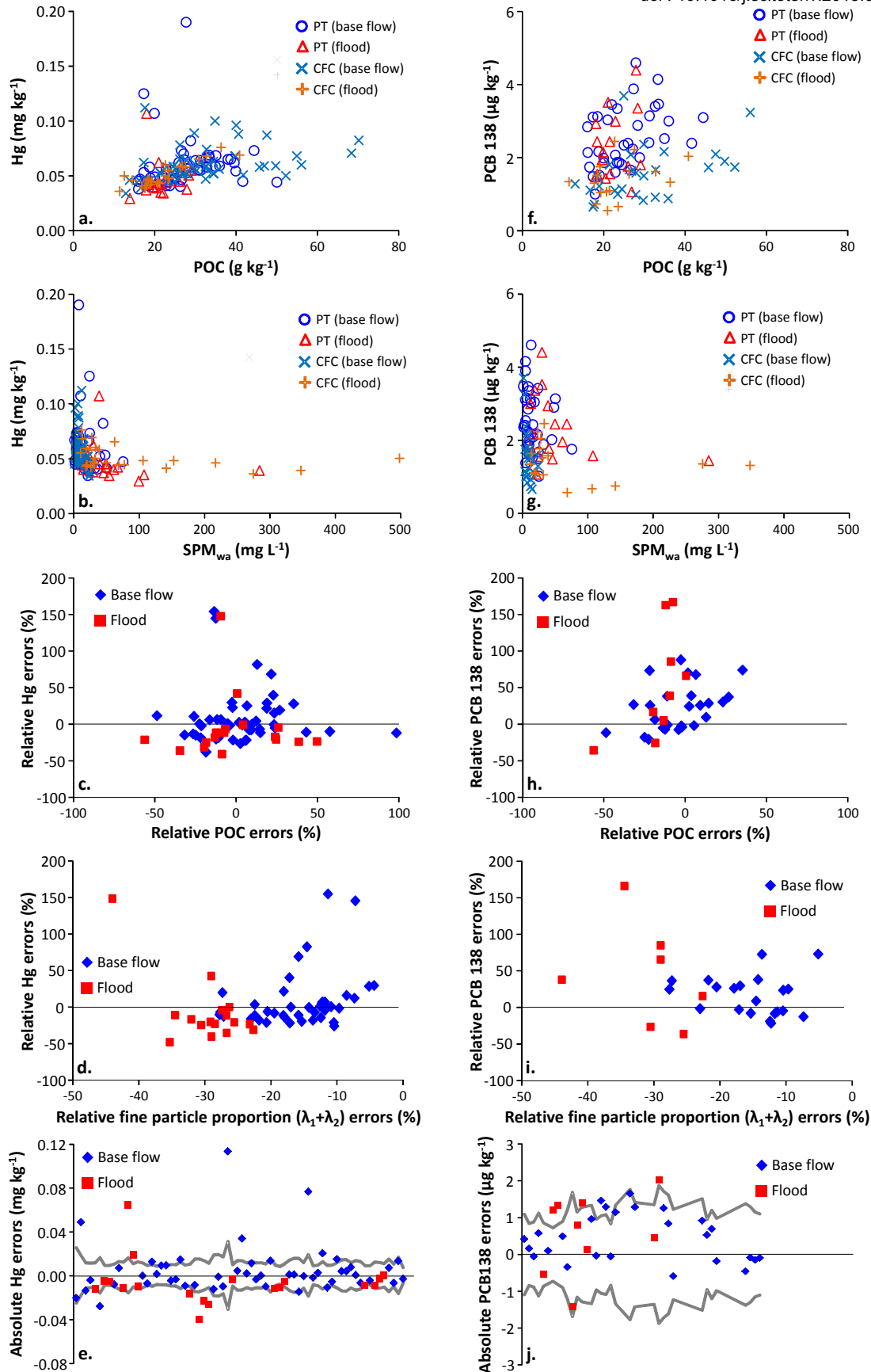


Figure 8: Trends in Hg and PCB 138 concentrations measured in SPM samples collected by PT and CFC at the Jons station from August 2012 to July 2016: (a) Hg concentrations vs. POC concentrations; (b) Hg concentrations vs. weighted average SPM concentrations; (c) relative Hg errors vs. relative POC errors; (d) relative Hg errors vs. relative fine particle proportion ($\lambda_1 + \lambda_2$) errors; (e) comparison of absolute Hg concentration errors with analytical errors (grey lines show estimated maximum errors due to analytical errors; data are ordered by sampling date). Same plots are shown for PCB 138 (f, g, h, i, j).

# test	Section	Description of the test	Type of test	p value	Conclusion
#1	3.2	λ_2 : PT vs. CFC samples	Wilcoxon	0.149	not different
#2	3.2	λ_1 : PT vs. CFC samples	Wilcoxon	< 2.2E-16	different
#3	3.2	λ_3 : PT vs. CFC samples	Wilcoxon	< 2.2E-16	different
#4	3.2	$\lambda_1+\lambda_2$: PT vs. CFC samples	Wilcoxon	< 2.2E-16	different
#5	3.3	POC : PT vs. CFC samples	Wilcoxon	0.2678	not different
#6	3.3	Hg : PT vs. CFC samples	Wilcoxon	0.1677	not different
#7	3.3	correlation between PCB 101, PCB 138, PCB 153 and PCB 180 (in all samples)	Kendall	all p-values : < 2.0E-08	positive correlations; Kendall corr.: 0.37 - 0.67
#8	3.3	PCB 138 : PT vs. CFC samples	Wilcoxon	0.289	not different
#9	4.1	λ_3 in CFC samples : base vs. flood periods	Wilcoxon	0.665	not different
#10	4.1	λ_3 in PT samples : base vs. flood periods	Wilcoxon	2.9E-08	different
#11	4.1	$\lambda_1+\lambda_2$ error : base vs. flood periods	Wilcoxon	7.5E-08	different
#12	4.2.1	correlation between SPM _{wa} and POC (in all samples)	Kendall	9.0E-15	negative correlation; Kendall corr.: -0.44
#13	4.2.1	POC error : distribution test	Shapiro-Wilk	0.845	normal distribution
#14	4.2.2	correlation between POC and Hg (in all samples)	Kendall	4.9E-15	positive correlation; Kendall corr.: 0.44
#15	4.2.2	Hg in PT samples : base vs. flood periods	Wilcoxon	2.9E-04	different
#16	4.2.2	Hg in CFC samples : base vs. flood periods	Wilcoxon	0.0047	different

Table 1: Statistical tests used for data comparison (non-parametric test of Wilcoxon), correlation determination (non-parametric test of Kendall) and normal distribution evaluation (Shapiro-Wilk test). For each test, the paragraph section and a brief description of the test are indicated. The result of each test is indicated by the p-value and a brief conclusion is given on the basis of a significance level of 0.05.

	PCB 101	PCB 138	PCB 153	PCB 180
PCB 101	1.00			
PCB 138	0.52	1.00		
PCB 153	0.59	0.67	1.00	
PCB 180	0.43	0.37	0.46	1.00

Table 2: Kendall correlation coefficients between concentrations of PCB 101, PCB 138, PCB 153 and PCB 180 measured in SPM samples collected by PT and CFC (not calculated for PCB 28, PCB 52 and PCB 118 as quantified in less than 50% of samples; concentrations below the LOQ were excluded). For all PCB couples, the p-values of the Kendall test were largely under 0.05 showing strong correlations between PCB concentrations.

Periods	Hg (kg)		PCB 138 (kg)		Difference PT vs. CFC	
	PT	CFC	PT	CFC	Hg	PCB138
annual : 2013	35.2	37.7	2.16	1.79	-7%	19%
annual : 2014	25.8	30.2	1.25	1.17	-16%	7%
annual : 2015	38.5	42.5	1.54	0.94	-10%	48%
flood period : 09/04 - 22/10/2013	19.9	16.8	0.98	0.90	17%	9%
dry period : 07/05 - 22/12/2015	10.7	10.4	0.30	0.25	3%	18%

Table 3: Hg and PCB 138 fluxes estimated at the Jons Station for different periods using PT and CFC contaminant concentrations and associated percentage differences.

- Particle traps (PTs) collect coarser particles than centrifugation (CFC) reference
- Hg and PCB differences between PT and CFC come mainly from analytical uncertainties
- PTs allow integrating variable contaminant concentrations during their deployment
- PTs are a reliable SPM sampling tool to assess contaminant fluxes at annual scale

